

**MEASUREMENT OF TRANSPORT PROPERTIES FOR THE DRIED  
LAYER OF COFFEE SOLUTION UNDERGOING FREEZE DRYING**

Yasuyuki Sagara , Jum-ichi Ichiba  
Department of Agricultural Engineering  
Faculty of Agriculture  
The University of Tokyo  
Yayoi 1-1-1, Bunkyo-ku, Tokyo 113

**Key Words and Phrases:** freeze-drying; coffee solution; thermal  
conductivity; Permeability;

**ABSTRACT**

A mathematical model has developed to determine the thermal conductivity and permeability for the dried layer of liquid sample undergoing sublimation dehydration. A microcomputer-based automatic measurement system has developed for the data acquisition as well as determination of these transport properties applying the drying data to the model. Aqueous solutions of 29-45 % soluble coffee solid were freeze dried under drying conditions used in commercial operations.

Thermal conductivity decreased in proportion to the porosity of the dried layer, and its temperature and pressure dependences were not appeared. The permeability increased with increasing the porosity, pressure and temperature of the dried layer. The results indicated that in commercial operations the solute concentration is one of the critical processing factors since this factor decisively governs the structure of a solute matrix formed during freezing of coffee solutions and the transport properties mainly depend upon the nature of this structure during drying.

## INTRODUCTION

Freeze drying has had a great impact upon the production of dehydrated food because of the superior quality of the product obtained and promises continued expansion of the number of applications. However, the process is only feasible if the cost of production can be lowered by optimum plant operations. Since the rate of freeze drying is limited by heat and mass transfer rates across a dried material which surrounds the frozen portion of product, the thermal conductivity and permeability of the dried layer and the effects of processing factors on these transport properties are fundamental information to determine the drying rate. Various methods, both transient and steady state, have been used to determine the transport properties of freeze dried food. The transient method used in this study based on a quasi-steady-state analysis of actual drying data, and was described by Lusk et al.(1), Massey and Sunderland(2), Hoge and Pilsworth(3), Stuart and Closset(4), Bralsford(5), Gaffney and Stephenson(6) and Sandall et al.(7). However, available literature on the transport properties for the dried layer of coffee solution was limited. Quast and Karel(8) reported the permeabilities for 20-30 % coffee solutions. Sagara and Hosokawa(9) determined the thermal conductivity and permeability of 2-30 % solutions at constant surface temperatures ranging from 20 to 53°C under the usual pressure range of commercial freeze dryers. However, economic consideration of freeze drying process make it desirable to prepare a concentrated solution of 30-50 % prior to freeze drying. Values of transport properties for this concentration range have not been measured systematically, and the data for freeze drying characteristics were not appeared in the literature.

The objectives of this work were a) to measure both freeze drying characteristics of coffee solution in a concentrated form, and b) to determine the thermal conductivity and permeability of the dried layer

in connection with controllable factors such as the solute concentration, temperature and vapor pressure for the dried layer.

Coffee solutions of 29-45 % were freeze dried at constant sample surface temperatures ranging from  $-7 - 70$  °C under the chamber pressure range of 7-12 Pa using radiant heating upon the sample surface. The transport properties of the dried layer were determined by applying the drying data to a model based on heat and mass transport in the sample, and then the effects of processing parameters on transport properties as well as the drying rate were discussed in connection with the freezing and freeze drying operations.

### THEORETICAL MODEL

A model used to determine the thermal conductivity and permeability of the dried layer is described next and shown in Fig.1.

The sample is assumed to have the geometry of a semi-infinite slab and the dried layer is separated from the frozen layer by an infinitesimal sublimation interface retreating uniformly from the sample surface. The assumption of infinitesimal sublimation front was based on the fact that a sharp sublimation zone had been observed to separate the completely dried layer and the frozen layer in the previous experiments (9), and also this has been validated for some applications by Sandall et al.(7) and Ma and Peltre (10). In addition, it is assumed that drying proceeds under quasi-steady-state condition; that is, the movement of sublimation front and the changes in temperature as well as pressure within the sample are negligible during calculation. Dyer and Sunderland (11) showed that this assumption results in an error of about 2 percent, and so this assumption is generally quite good for the case of radiant heating. The bottom of the sample is insulated while the surface is exposed to a evacuated space at the temperature  $\theta_0$  and pressure  $p_0$ . The insulated sample bottom may be considered the center line of a symmetric slab heated from both surface and bottom. Since the

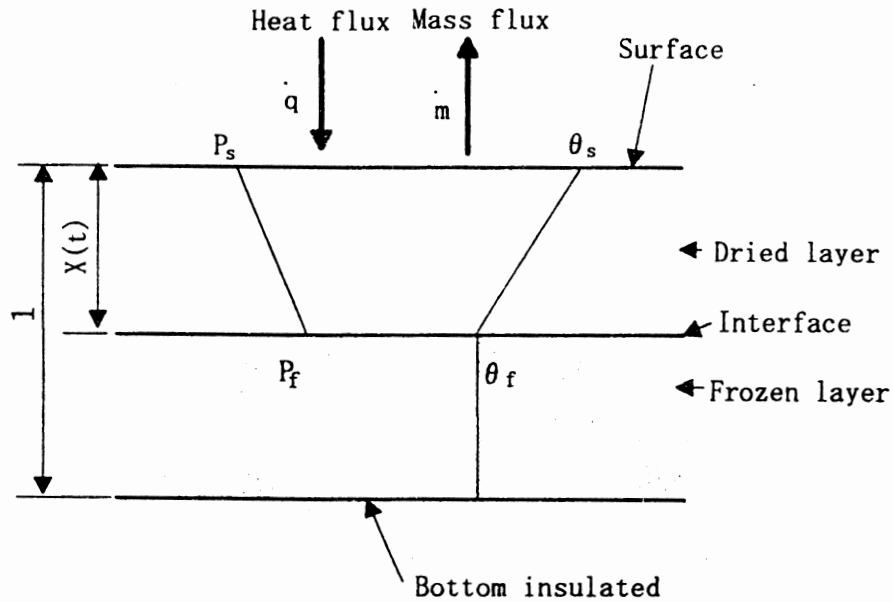


FIGURE 1 Freeze-drying model for transport properties analysis

thermal conductivity of the frozen layer is 20-50 times greater than that of the dried layer, the temperature of the frozen layer can be supposed to be uniform and same as that of sublimation front.

The expression for the rate of heat transfer across the dried layer is taken from Massey and Sunderland (2);

$$\dot{q} = \frac{\lambda}{x(t)} (\theta_s - \theta_f) - \dot{m} \int_{\theta_f}^{\theta_s} c_p d\theta \quad (1)$$

The specific heat of water-vapor  $c_p$  was assumed constant and equal to the value of water-vapor. The first term on the right side of the equation represents the heat conducted across the dried layer and the second term the energy absorbed by the water-vapor flowing through the dried layer. A linear distribution of temperature within the dried layer was

assumed in the calculation of transport properties. Similarly, the mass flux may be expressed as

$$\dot{m} = \frac{KM_w}{RTx(t)}(p_f - p_s) \quad (2)$$

where  $K$  is the permeability between the sample surface and the sublimation front with the partial pressure of water-vapor  $p_f$ .

An expression for the equilibrium vapor pressure (torr) of pure ice as a function of temperature is given by I.C.T. (12);

$$\log p_f = -2445.5646/T_f + 8.23121 \log T_f - 1.1677006T_f + 1.20514 \times 10^{-5} T_f^2 - 6.757169 \quad (3)$$

As heat supplied across the dried layer may be considered to be dissipated as the latent heat of sublimation, the sublimation front acts as the heat sink, which can be represented by

$$\dot{q} = \dot{m} \Delta H \quad (4)$$

The mass transfer rate can be related to the drying rate as

$$\dot{m} = \rho_w l \left( -\frac{dX}{dt} \right) \quad (5)$$

where  $\rho_w$  is the density of ice or frozen liquid and  $X$  is the fraction of water still remained in the sample. Fig. 2 shows the grouping of water within the sample during sublimation dehydration process. According to this configuration, the fraction of  $X$  be expressed as

$$X = (m_d + m_f + m_w) / m_0 \quad (6)$$

where  $m_d$  is the residual water as the sample is fully dried,  $m_f$  is the water contained in the frozen layer,  $m_w$  is the water-vapor flowing

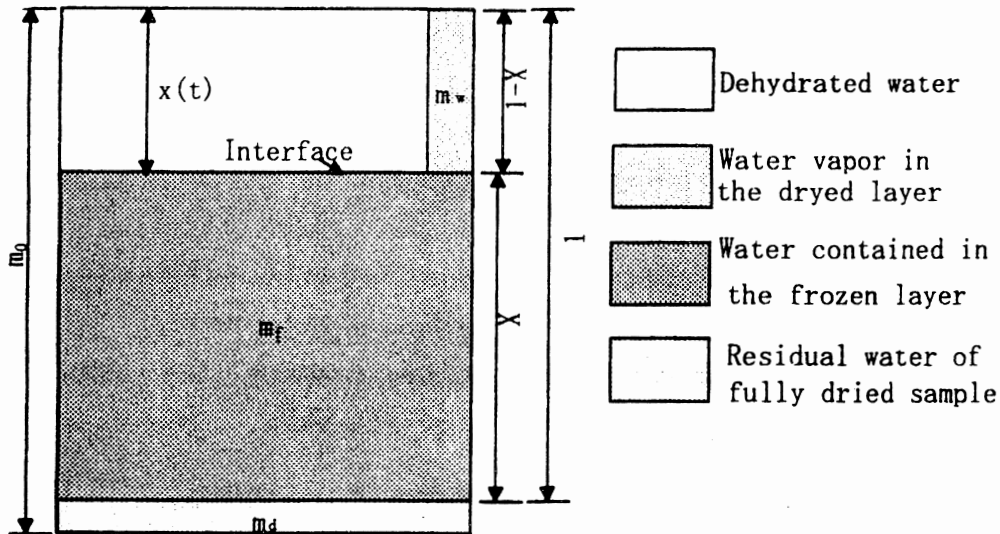


FIGURE 2 Grouping of water within the sample undergoing sublimation dehydration

through the dried layer, and  $m_0$  is the initial water. By neglecting the mass of water-vapor as well as residual water which does not take part in deciding the position of interface the value of  $X$  is approximated by

$$X = m_f / (m_0 - m_d) \quad (7)$$

If it is assumed that complete drying except the residual water occurs during the retreat of the frozen layer, the thickness of the dried layer  $x(t)$  may be expressed in term of the fraction of water remaining,  $X$ ;

$$x(t) = (1 - X) l \quad (8)$$

Substitution of equation (5) into equation (4) gives

$$\dot{q} = \rho_w l \Delta H (-dX/dt) \quad (9)$$

Following a substitution of equation (8) into equations (1) and (2), equations (1) and (9) may be combined to give the fraction of dehydrated water;

$$(1-X) = \frac{\lambda(\theta_s - \theta_f)}{\rho_w l^2 \left( \Delta H + \int_{\theta_f}^{\theta_s} c_p d\theta \right) \left( -\frac{dX}{dt} \right)} \quad (10)$$

Similarly, from equations (2) and (5);

$$(1-X) = \frac{KM_w(p_f - p_s)}{\rho_w l^2 RT_f \left( -\frac{dX}{dt} \right)} \quad (11)$$

Equations (10) and (11) were used to test drying rate data for conformity to the model and to deduce the transport properties from drying rate data. By rewriting equations (10) and (11), the following equations for the thermal conductivity and permeability are obtained, respectively;

$$\lambda = \alpha \rho_w l^2 \left( \Delta H + \int_{\theta_f}^{\theta_s} c_p d\theta \right) \quad (12)$$

$$K = \beta \rho_w l^2 RT_f / M_w \quad (13)$$

where,

$$\alpha = \frac{(1-X)}{(\theta_s - \theta_f) / (-dX/dt)}, \quad \beta = \frac{(1-X)}{(p_s - p_f) / (-dX/dt)} \quad (14)$$

In this study, the average values of transport properties in quasi-steady state periods were determined with the average values of  $\alpha$  and  $\beta$  in these periods.

## EXPERIMENTAL

### Experimental freeze dryer

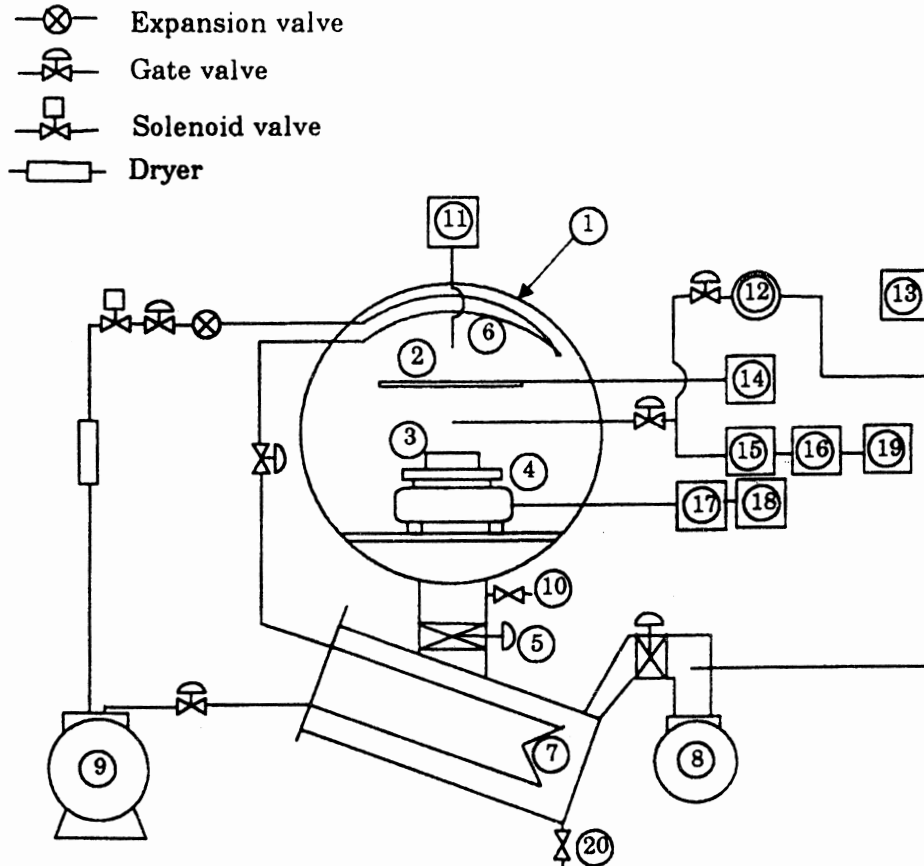
The vacuum chamber and adjacent parts of the apparatus are illustrated in Fig.3. The vacuum chamber was a cylindrical, thermally insulated iron enclosure of 92.2 mm in inside diameter by 470 mm long, with a Plexiglas door of 30 mm thick. A rotary vacuum pump was connected through a external condenser and a main valve to the lower part of the vacuum chamber. A diffusion pump was used to evacuate a diaphragm-type pressure sensor head and adjust its zero-point. Both internal and external condensing systems were used to collect and freeze water-vapor sublimed from the sample and prevent moisture from reaching the vacuum pump. A refrigerator for these condensers is a 1.5 kW (R-22 Refrigerant) air-cooled condensing unit with sufficient capacity to reduce the condenser-coil surface temperature to  $-45^{\circ}\text{C}$ . Radiant heat was supplied by electrically heated plate located above the sample surface. Then the sample surface temperature was controlled with the PID controller by regulating the electrical power to the radiant heater.

### Automatic measurement system

The weight loss of the sample was followed by supporting a sample holder on a electric balance located in the center of the vacuum chamber. This was accomplished by separating a part of road cell from an indicator containing electric circuits. The chamber pressures were measured with both Pirani- and diaphragm-type analyzers.

The system can be programmed to display both real-time parameters pertinent to the drying characteristics of the sample tested as well as corresponding operating conditions and changes in transport properties against drying time. The drying characteristics illustrated on a CRT display consisted of the changes in transport properties, sample





1. Vacuum chamber
2. Radiant heater
3. Sample
4. Electric balance
5. Main valve
6. Internal condenser
7. External condenser
8. Rotary Vacuum pump
9. Refrigerator (Condensing unit)
10. Leak valve
11. Pirani vacuum gage
12. Diffusion pump
13. Thermo-recorder
14. Heater temperature controller
15. Diaphragm-type pressure sensor
16. Pressure indicator
17. Weight indicator
18. Weight recorder
19. Pressure recorder
20. Drain valve

FIGURE 3 Schematic diagram of experimental freeze-dryer

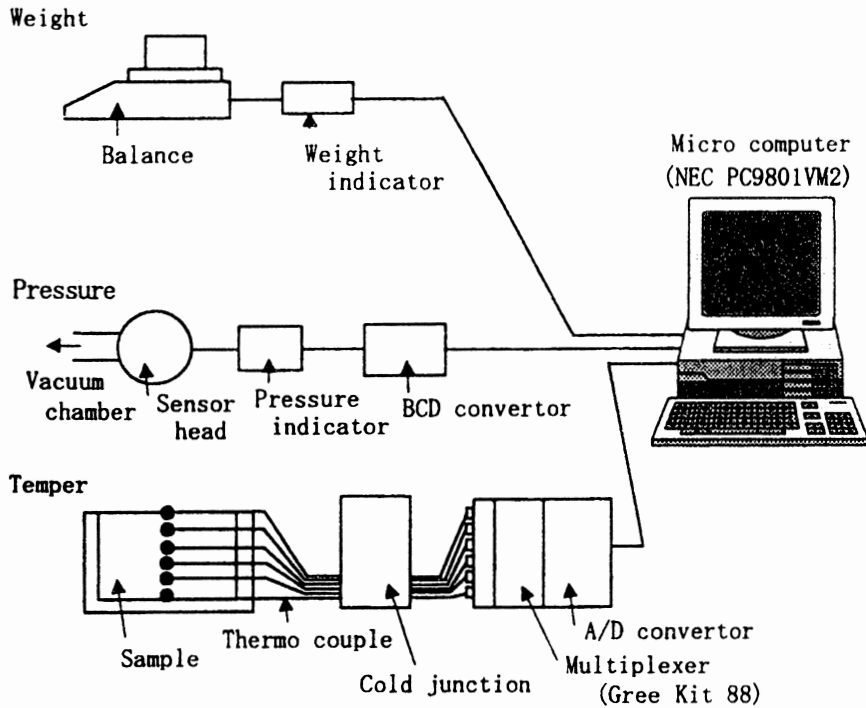


FIGURE 4 Automatic measurement system for transport properties of food sample during freeze-drying

weight, drying rate, position of sublimation front and temperature distribution in the sample while operating conditions included the surface temperatures of the heater and condenser as well as the chamber pressure. All of these data were stored into a floppy disk every two minutes in order to print the data against the drying time.

#### Sample holder

The sample holder and measuring locations of temperature in the sample were shown in Fig.5. The sample holder was a Plexiglas dish of 70.5 mm in inside diameter and 25 mm in height. To promote one-dimensional freezing and freeze-drying, a fiber-glass insulation was placed around the side of the sample holder. After the sample was frozen

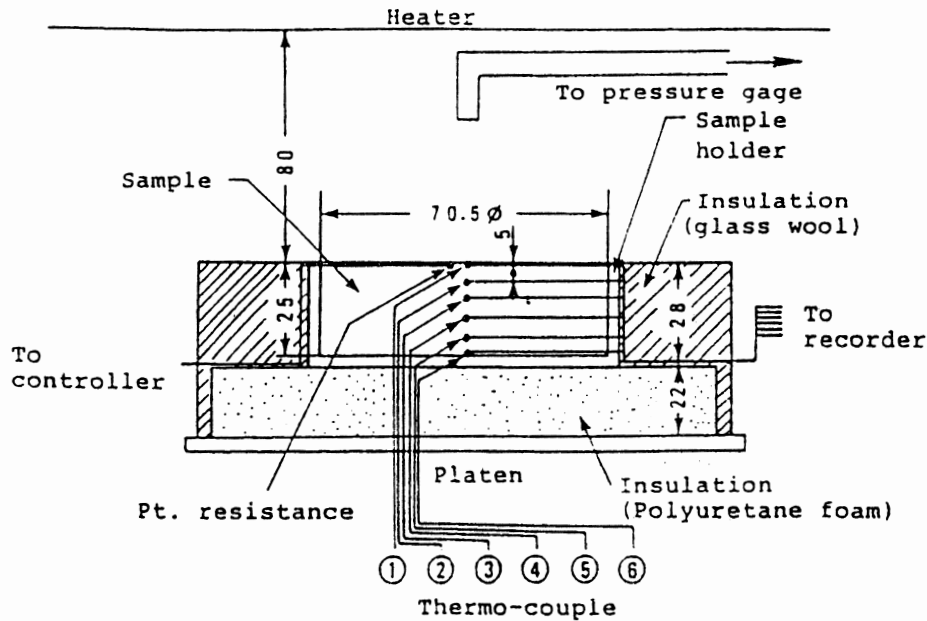


FIGURE 5 Sample holder for liquid and granular materials

the sample holder was placed on a 50 mm by 150 mm square piece of Polyuretane foam fixed on the platen. All the exposed surfaces of insulating materials were covered with reflecting aluminium foil to reduce radiant heat transfer to the side and bottom of the sample holder.

Six thermocouple probes made from 0.2 mm copper-constantan wire were permanently placed in the center of the sample holder and equally spaced from the exposed surface of the sample, and made it possible to make temperature measurements at the same points in the sample from run to run. The thermocouple junctions for measuring and controlling the sample surface temperature were placed just under the exposed surface of the sample to ensure a meaningful surface temperature reading, and the probes were run along the surface to the side of the sample holder to provide an isothermal path to minimize conduction errors along these probes. The leads were also shielded from the heater

by passing them through the insulation in order to prevent direct radiant heat transfer to the wire.

### Procedure

The samples of 29-45 % aqueous solutions of instant soluble coffee solid were used and each sample was prepared for freeze drying in the same manner. The powder was thoroughly mixed with distilled water and allowed to cool to room temperature. Then it was frozen from the bottom of the sample holder using a freezing plate cooled with freezing-mixture (Dry ice-Ethanol). Freezing continued until uniform temperature of the sample was obtained, resulting in a relatively fast freezing rate with crystallization period under 30 min. and a final sample temperature below  $-65^{\circ}\text{C}$  within 60 min. From this manner, a capillary-type solute matrix with its grain orientation parallel to direction of heat and mass transfer. As described later an expanded portion of frozen sample contained a concentrated film (See Fig. 6) was scraped with a knife after freezing. The frozen sample was then transferred into the vacuum chamber, freeze drying continued until constant weight of the sample was obtained. The water content of the dried sample was determined by Karl Fisher titration method.

## RESULTS AND DISCUSSION

### Drying characteristics

Table 1 presents the drying conditions for the coffee samples used in this study. The sample temperatures and vapor pressures indicate the average values obtained during quasi-steady-state periods and these values were used to calculate the transport properties. The vapor pressure at the sublimation front  $p_f$  was calculated from the sublimation temperature, which was measured with the thermocouple nearest

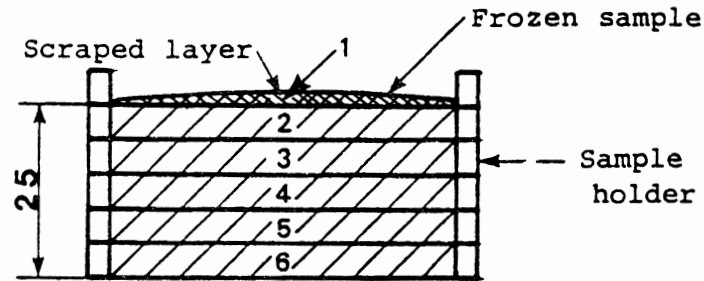


FIGURE 6 Schematic diagram of frozen sample

TABLE 1 Drying conditions for the Coffee Samples

Sample No.	Concentration (% w. b.)	Sample Temperature (°C)		Vapor Pressure (Pa)		Heater Temperature (°C)		Drying time (h)
		$\theta_s$	$-\theta_f$	$p_s$	$p_f$	$\theta_{hmax}$	$\theta_{hmin}$	
1*	28.5	59.0	21.3	11.0	91.7	260.0	98.2	43.3
2*	33.7	29.1	21.2	6.9	92.6	138.7	35.5	44.7
3*	38.6	0.0	22.2	10.4	83.8	88.1	0.0	67.4
4*	40.2	-6.5	21.7	8.1	88.4	67.3	-6.3	59.1
5	40.3	19.1	21.9	9.2	86.5	66.2	19.3	38.0
6	40.4	24.3	21.3	9.3	91.7	74.5	24.3	36.8
7	40.4	28.9	22.2	12.4	84.0	77.4	31.6	29.2
8	40.6	35.2	21.3	9.1	91.7	77.4	35.5	27.7
9	40.5	49.7	18.9	9.9	115.5	90.0	48.3	45.3
10	39.9	54.5	20.3	9.1	101.0	119.7	54.8	22.3
11	40.3	60.5	18.2	10.1	123.5	128.7	58.5	25.1
12	40.0	39.5	21.3	8.7	91.7	83.6	39.3	32.0
13	40.0	70.7	18.6	10.0	118.9	130.7	68.0	22.4
14	45.0	19.6	20.3	9.5	101.0	76.2	21.3	32.0

Condenser temperature  $\theta_c = -43.1 \sim -45.4$  (°C)

\* without scraping

to the sublimation front within the frozen layer. Heater temperature represents the maximum or minimum value appeared during drying process.

The physical properties for the initial and dried samples were presented in Table 2. Porosity, volume, and density were assessed from cumulative composition using 0.625 specific volume for pure coffee solubles (14). The relationship between solute concentration and initial

TABLE 2 Physical properties of initial and dried samples

Sample No.	Volume (cm <sup>3</sup> )	Porosity (-)	Mass (g)				Water Content (%w. b.)		Density (g/cm <sup>3</sup> )				
			Vo	Ψ	mo	md	ms	mw	wo	wd	ρo	ρd	ρw
1	105.0	0.80	118.55	34.72	9.90	108.65	71.5	2.61	1.129	0.331	0.807		
2	103.6	0.76	120.19	41.92	14.14	106.05	66.3	3.28	1.160	0.405	0.769		
3	102.5	0.71	123.00	50.12	19.33	103.67	61.4	5.36	1.200	0.489	0.737		
4	103.1	0.69	125.57	54.05	21.73	103.84	59.8	6.61	1.218	0.524	0.728		
5	92.8	0.70	111.56	46.79	18.84	92.72	59.7	4.01	1.202	0.504	0.718		
6	92.9	0.70	111.30	46.50	18.77	92.53	59.6	3.39	1.198	0.501	0.714		
7	92.5	0.70	111.01	46.56	18.82	92.19	59.6	3.62	1.200	0.503	0.715		
8	92.3	0.70	110.54	46.30	18.81	91.73	59.4	3.03	1.198	0.502	0.711		
9	93.4	0.70	111.36	46.21	18.73	92.63	59.5	2.31	1.192	0.495	0.709		
10	93.9	0.70	111.82	46.01	18.36	93.46	60.1	3.03	1.191	0.490	0.716		
11	93.8	0.70	111.96	46.39	18.70	93.26	59.7	2.73	1.194	0.495	0.713		
12	94.0	0.70	111.85	45.77	18.30	93.55	60.0	2.27	1.190	0.487	0.714		
13	94.1	0.70	111.71	45.57	18.25	93.46	60.0	1.83	1.187	0.484	0.712		
14	92.8	0.65	114.41	53.81	24.23	90.18	55.0	4.27	1.233	0.580	0.678		

density obtained is consistent with that used in commercial plants operations.

It was observed that during freezing the sample a concentrated film of solute developed at the free surface of the sample and this film forms an effective water-vapor barrier, which causes melting or puffing in the sample for the reason that the temperature of the frozen layer rises until the melting or collapse temperature is reached. The samples numbered from 1 to 4 were dried without scraping after freezing. As shown in these samples, the solute concentration exerts a great influence on the sample surface temperature. For example, the surface temperature of about 40 % solution was not be allowed to heat to above -6.5 °C to avoid the puffing in the sample. Table 3 shows the concentration distribution in the frozen sample, which was determined by Karl Fisher titration method using three samples of about 40 % solution, and Fig.6 illustrates its measuring locations. The concentration of the surface layer which contains the film was determined to be about 1 %

TABLE 3 Solute concentration values for frozen samples

Specimen No.	Concentration (% w. b.)		
	Sample No. 1	No. 2	No. 3
1	41.4	41.8	41.9
2	40.4	40.8	41.1
3	40.4	40.8	41.0
4	40.4	40.8	41.2
5	—	40.8	41.5
6	40.5	40.7	41.3

higher than other layers. Flink(14) mentioned the existence of a surface film or crust resistance to mass transfer, and a sample whose frozen surface was scraped prior to drying had a significantly higher permeability. He also interpreted that in most solutions this is due to the concentration of carbohydrates, and suggested several methods for removing the surface layer effect. According to these suggestions, an expanded portion was scraped with a knife after freezing, and the data for the samples of 40 % solutions indicate that the scraped volume is about 10 per cent of the initial. This treatment was found to be successful for removing the surface film effect and thus the surface temperatures, which had been limited as low as  $-6.5^{\circ}\text{C}$  for 40 % solution, were allowed to heat up to  $70^{\circ}\text{C}$  or higher, resulting in a reduced drying time by one-third as shown in sample No.13.

A typical freeze drying characteristics and corresponding drying conditions are shown in Fig.7. The former consists of the change in sample weight, drying rate, temperature distribution in the sample while the latter includes the surface temperatures of the heater and internal condenser coil as well as the chamber pressure. The sample surface temperature increased until it approached the control temperature and then remained constant. A uniform temperature in the frozen

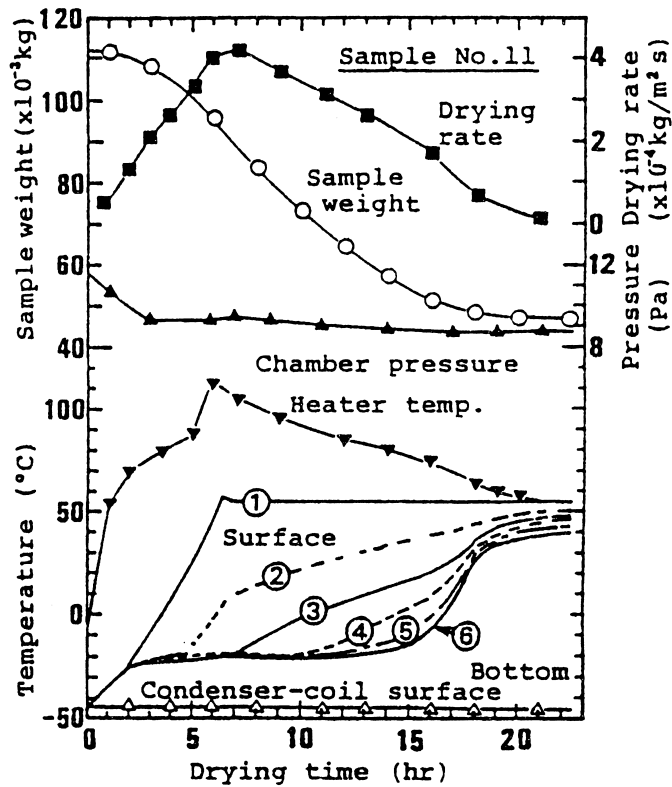


FIGURE 7 Experimental data obtained during of 25mm layer of a 40.3% aqueous solution of soluble coffee at surface temperature 54.5 °C

layer was observed during most of runs and the assumption employed in the model was confirmed to be satisfied. The temperature at any given location in the sample appeared to reach a minimum value just before it began to rise and then rose toward the surface temperature indicating the passage of retreating sublimation front. The temperature of sublimation front was found to decrease as the chamber pressure gradually decreased. Same behavior was observed for all samples used and this indicates the fact that the drying process was heat transfer controlled. For example, as shown in sample No.5-13, a variation in surface temperature of 19.1 to 70.7 °C has little effect on the interface



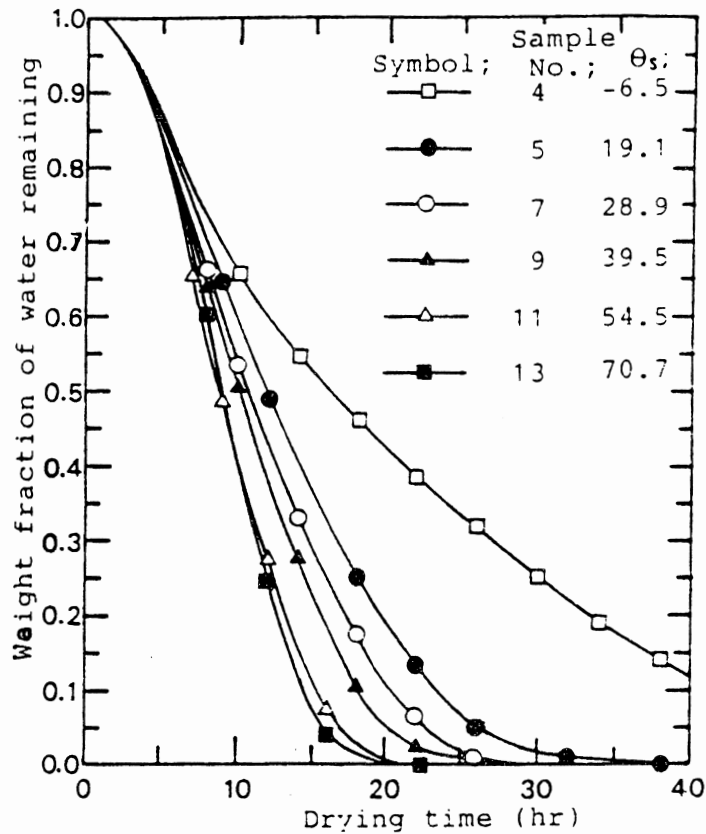


FIGURE 8 Experimental drying curves of 40% solutions at various surface temperatures

temperature; namely, the drying rate is much more sensitive to the thermal conductivity of the dried layer than to the permeability.

The weight loss curves of about 40 % solutions at various surface temperatures and corresponding drying rate curves are shown in Fig.8 and Fig.9, respectively. Drying time decreased with increasing the sample surface temperature as expected. The drying rate increased until the sample surface temperature reached its control temperature and after showing the maximum value it decreased gradually indicating an increasing resistance of the dried layer to heat transfer. Increasing the sample surface temperature led to an increase in the maximum value of

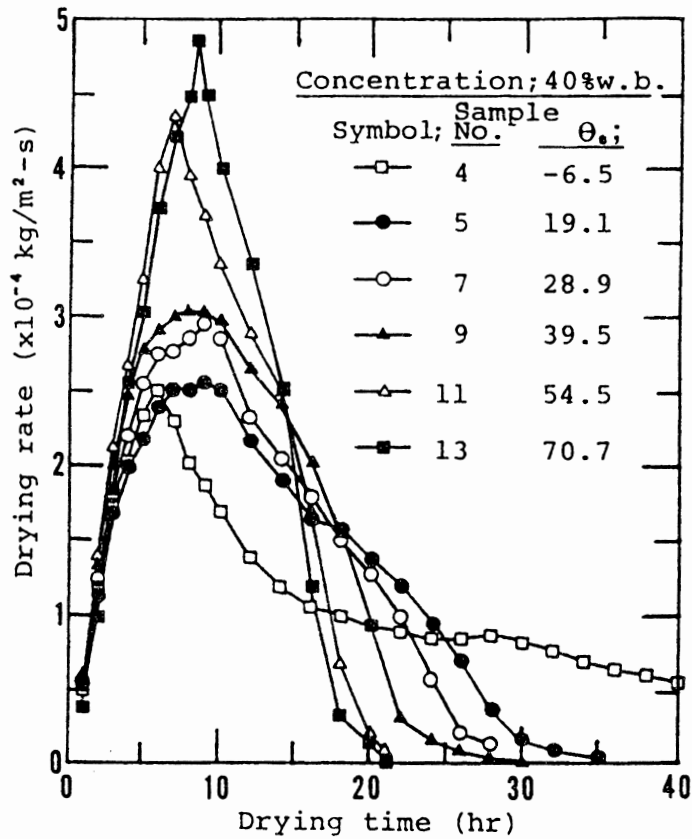


FIGURE 9 Drying rate curves of 40% solutions for various surface temperatures

the drying rate. The sample without scraping (See sample No.4) required an extremely longer drying time compared with other samples for reason that the sample surface temperature had to be kept lower as described above.

#### Transport properties

The thermal conductivity and permeability of the dried layer are given in Table 4. Because the sample surface temperature did not instantly jump to a constant value at the start of drying as shown in

TABLE 4 Thermal conductivity and permeability for coffee solutions

Sample No.	Concentration	Porosity	Temperature*	Pressure*	Thermal conductivity	Permeability
	(% w. b.)	(-)	(°C)	(Pa)	(W/m-K)	( $\times 10^{-10}$ m <sup>2</sup> /s)
	C	( $\Psi$ )	$\theta$	p	$\lambda$	K
1	28.5	0.80	18.9	51.4	0.153	0.593
2	33.7	0.76	4.0	49.8	0.170	0.398
3	38.6	0.71	-11.1	47.1	0.241	0.293
4	40.2	0.69	-14.1	48.3	0.277	0.213
5	40.3	0.70	-1.4	47.9	0.197	0.419
6	40.4	0.70	1.5	50.5	0.209	0.460
7	40.4	0.70	3.3	48.2	0.196	0.555
8	40.6	0.70	7.9	50.4	0.208	0.562
9	40.5	0.70	15.4	62.7	0.203	0.585
10	39.9	0.70	17.1	55.1	0.210	0.540
11	40.3	0.70	21.2	66.8	0.203	0.649
12	40.0	0.70	9.1	50.2	0.202	0.554
13	40.0	0.70	26.1	64.5	0.195	0.625
14	45.0	0.65	-0.3	55.3	0.224	0.391

\* Average value for the dried layer

Fig.7, only drying data obtained during a quasi-steady-state period, which was appeared after the sample surface temperature reached the constant temperature, was applied to the model. During this period the ratio of heat flow density to mass was essentially constant indicating a constant temperature of the sublimation front.

The thermal conductivity for the sample without scraping was found to increase with increasing the solute concentration, and its value for about 40 % solution was about 20 per cent greater than those of scraped samples. Effects of temperature and pressure of the dried layer on thermal conductivity were not appeared definitely under experimental condition and the average of 40 % solutions was assessed to be  $0.203 \text{ W m}^{-1}\text{K}^{-1}$ . The results obtained in the present and previous studies show clearly that thermal conductivity is markedly affected by solute concentration or the porosity of the dried layer as shown in Fig.10. A linear relationship between thermal conductivity and porosity was

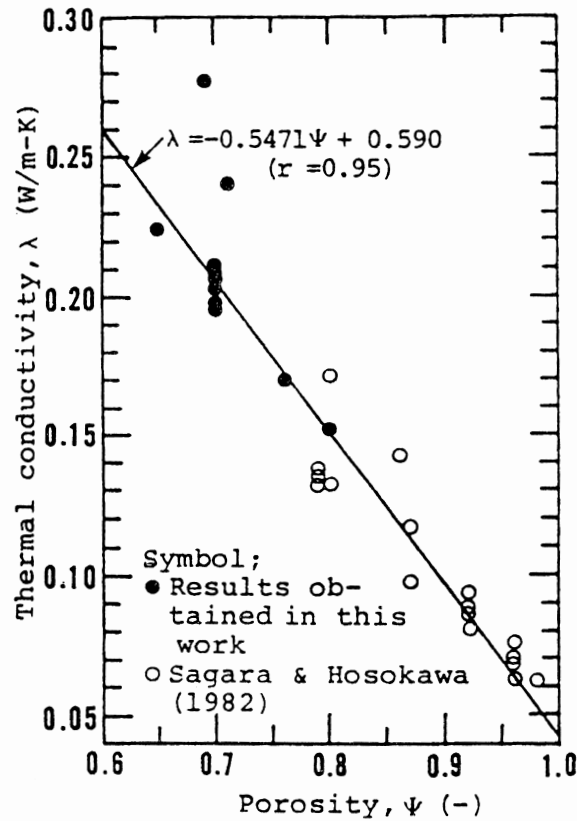


FIGURE 10 Thermal conductivity versus porosity

obtained and the equation for a regression line fitted to all of the data is also presented.

It was observed that in the samples dried without scraping a markedly low permeability was assessed as shown in sample No.4 and the effects of concentrated surface film on permeability was decreased with decreasing solute concentration as indicated in sample No.1-4. For all samples of about 40 % solutions whose surface layers scraped, the permeability was found to increase with the pressure and temperature of the dried layer as shown in Table 4. This behavior is in good agreement with Mellor and Lovett's theoretical investigations (16) based

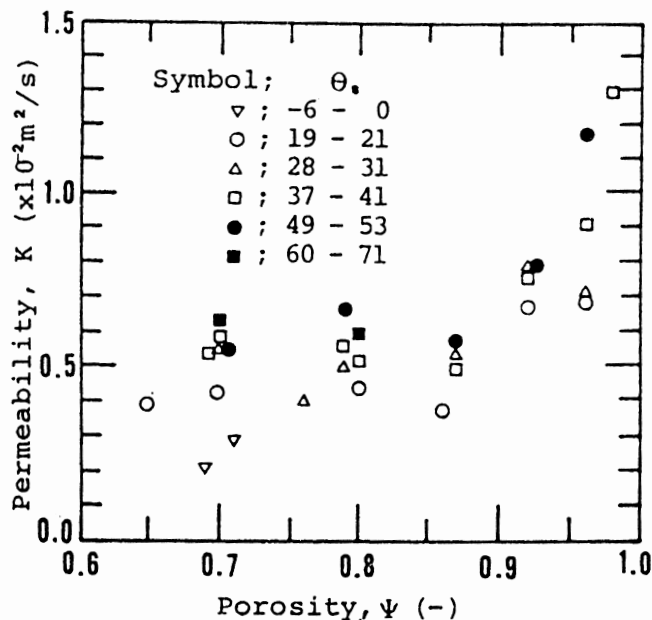


FIGURE 11 Permeability versus porosity for various surface temperatures

on the collision theory, and also with their experimental results obtained for several kinds of solutions.

The relationship between permeability and porosity at various sample surface temperature is shown in Fig.11. The data obtained in the previous work(9) are also plotted on the figure. Permeability was found to depend mainly on the porosity of the dried layer and then other factors such as temperature or pressure of it.

These results indicate that the transport properties mainly depend upon the structural nature of the dried layer and secondary on the operating factors such as pressure or temperature. In commercial plant operations the solute concentration is one of the critical processing factors since this factor decisively governs the structure of solute matrix formed during freezing of coffee solution and this structure is remained as that of the dried layer during sublimation dehydration process.

## REFERENCES

1. Lusk, G., Karel, M. and Goldblith, S.A., 1964, Thermal Conductivity of Some Freeze-Dried Fish, *Food Technology*, 18(10) pp. 1625-1628.
2. Massey, W.M. and Sunderland, J.E., 1967, Measurement of Thermal Conductivity during Freeze-drying of beef, *Food Technology*, 21(3A) pp. 90A-94A.
3. Hoge, H.J. and Pilsworth, M.N., *J. of Food Sci.*, 1973, Freeze-Drying of beef, *J. of Food Science*, 38 pp.841-848.
4. Stuart, E.B. and Closset, G., *J. of Food Sci.*, 1971, Pore Size Effect in the Freeze-Drying Process, *J. of Food Science*, 36 pp.388-391
5. Bralsford, R., 1967, Freeze-Drying of Beef, *J. of Food Technology*, 2 pp.339-363.
6. Gaffney, J.J. and Stephenson, K.Q., 1968, Apparent Thermal Conductivity during Freeze-Drying of a Food Model, *Trans. of ASAE*, 11(6) pp.874-880
7. Sandall, O.C., King, C.J. and Wilke, C.R., 1967, The Relationship Between Transport Properties and Rates of Freeze-Drying of Poultry Meat, *AIChE J.* 13(3) pp.428-438.
8. Quast, D.G. and Karel, M., 1968, Dry Layer Permeability and Freeze-Drying Rates in Concentrated Fluid Systems, *J. of Food Science*, 1(33) pp. 170-175.
9. Sagara, Y. and Hosokawa, A., 1982, Dry Layer Transport Properties and Freeze-Drying Characteristics of Coffee Solutions, *Proc. Third Int. Drying Symposium IDS '82, Birmingham*, pp.487-496
10. Ma, Y.H. and Peltre, P.R., 1975, Freeze-Dehydration by Microwave Energy Part 1 Theoretical Investigation, Part 2 Experimental Study, *AIChE J.*, 21(2) pp.335-350.
11. Dyer, D.F. and Sunderland, J.E., 1968, Heat and Mass Transfer Mechanisms in Sublimation Dehydration, *Trans. ASME, J. of Heat Transfer*, pp.379-384.

12. Nat. Res. Council of USA, International Critical Table, vol.3, McGraw-Hill, New York p210.
13. Flink, J.M., 1974, Properties of the Freeze-Drying "Scorch" Temperature, J. of Food Science, 39 pp.1244-1246.
14. Sivetz, M. and Desrosier, N.w., 1979, Coffee Technology, AVI. Westport, p551.
15. Sagara, Y., Kameoka, T. and Hosokawa, A., 1982, Measurement of Thermal Conductivity and Permeability of the Dried Layer During Freeze-Drying of Beef, J. of Soci. Agr. Machinery, Japan 44(3) pp.477-487.
16. Mellor, J.D. and Lovett, D.A., 1964, Flow of Gases Through Channels with Reference to Porous Material, Vacuum, 18 pp.625.